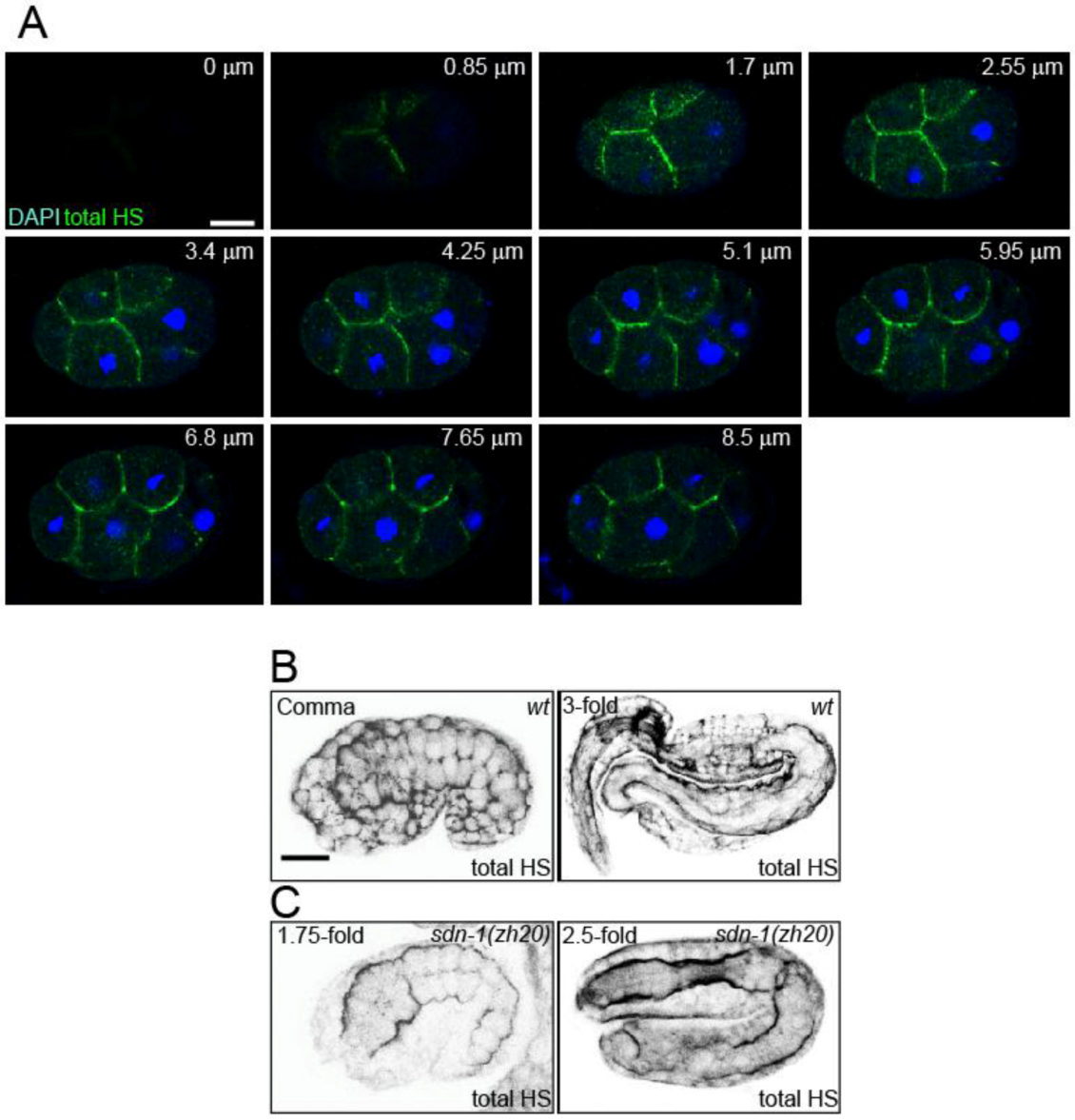

Figure S1. SDN-1 and additional HSPGs contribute to total HS at mid- to late embryonic stages

(A) Montage of confocal images of anti-HS (3G10) immunostaining in 8-cell stage embryo with DAPI (blue) counter staining. Total HS is present in the cell-cell interface, which is not visible in 3D projection image in Fig. 1Ae. (B, C) Single focal plane images of 3G10 immunostaining of wild type (B) and *sdn-1(zh20)* embryos (C), at comma-1.5 fold stage and 2-3 fold stage. In wild type embryos, HS is expressed on cell surfaces of most cells at the comma stage. In *sdn-1(zh20)* HS staining is absent from most cells apart from the basement membrane of the intestine and pharynx, indicating the existence of additional HSPGs at these stages. Scale bars: 10 µm.

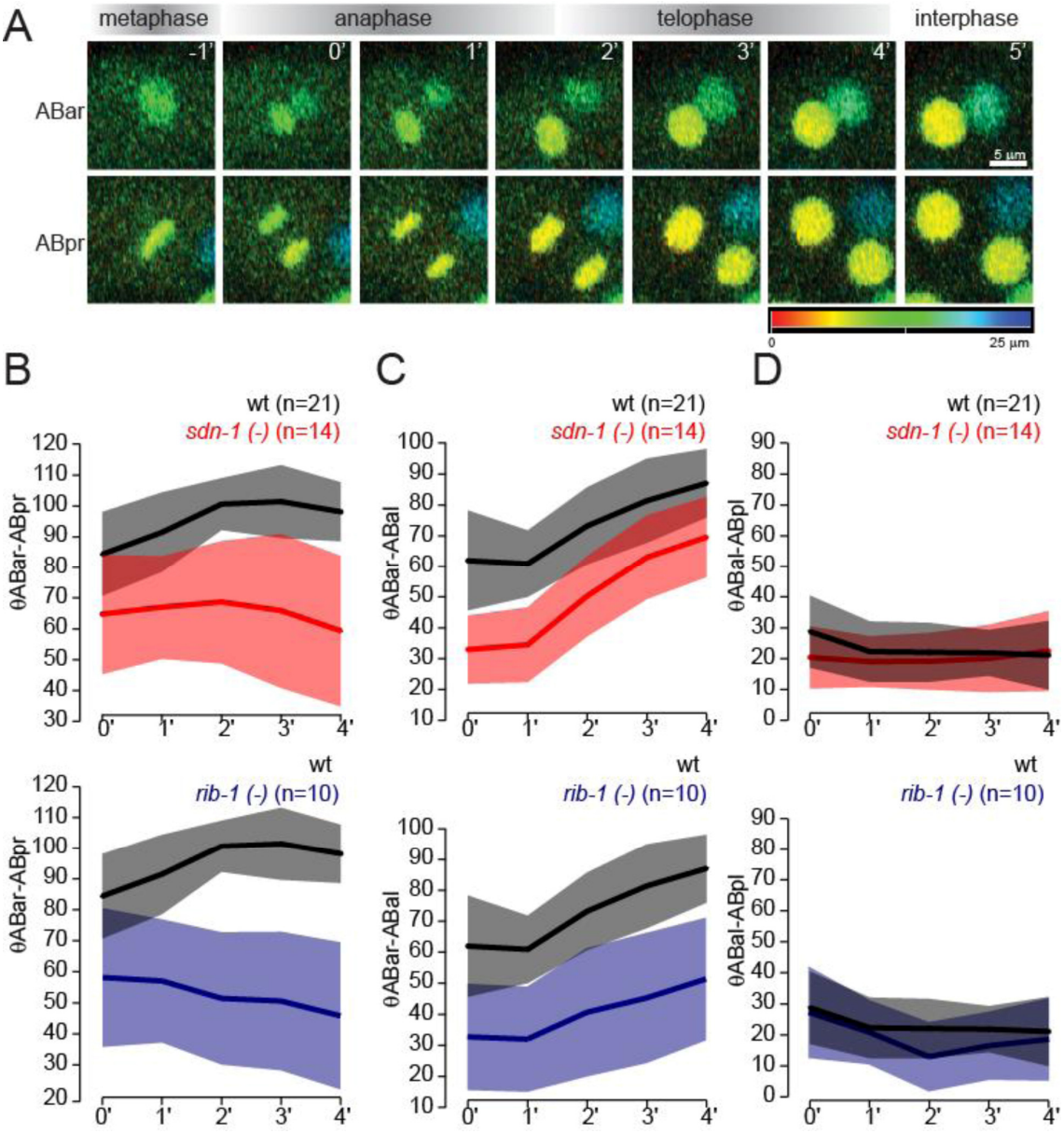

Figure S2. Loss of SDN-1 or HS synthesis affects ABar division orientation throughout the cell cycle

(A) Representative 3D reconstructed confocal images of HIS-72::GFP in ABar and ABpr during their divisions in wild-type embryos, color depth code. (B) Graphs of 3D division angle (*y*-axis) over time (*x*-axis, min relative to onset of anaphase). The angles (θ) of ABar division axes relative to the ABpr division axis (left panels) or to the ABal division axis (middle panels) are affected in the *sdn-1(zh20)* and *rib-1(tm516)* mutant throughout the cell cycle. The angles between ABal and ABpl division axes are unaffected (right panels). Mean angles are plotted as lines, shaded areas denote s.d.

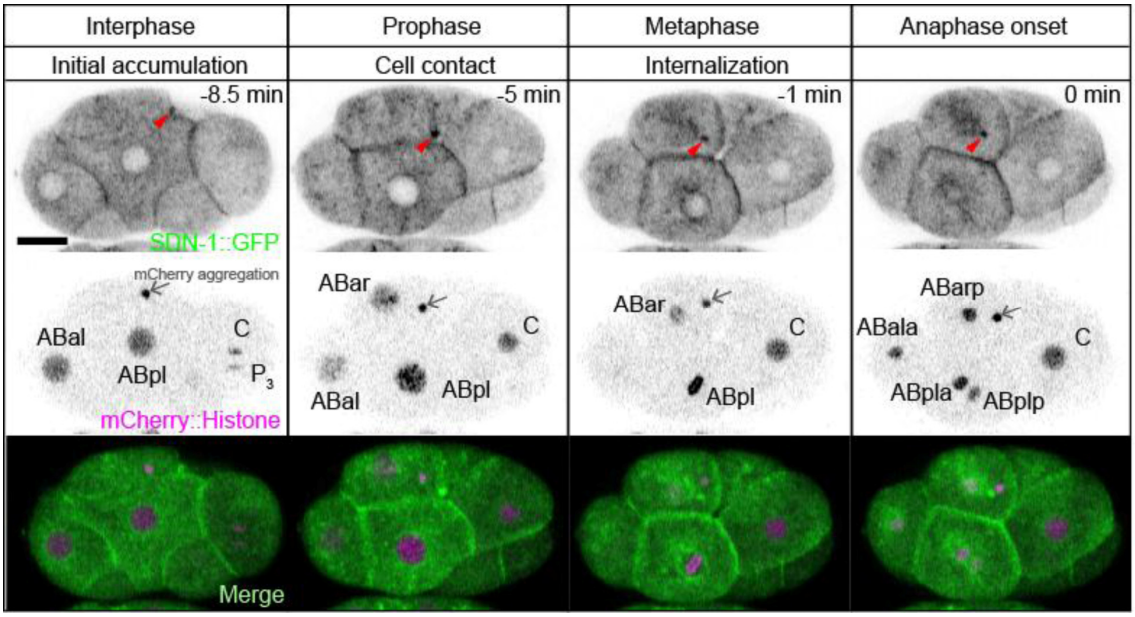

Figure S3. Pattern of SDN-1::GFP localization during the ABar cell cycle.

Projections of confocal z-stacks of a single embryo during ABar mitosis. SDN-1::GFP initially accumulates on the ABar cell surface (red arrowhead) during interphase (8.5 min before anaphase). SDN-1::GFP remains localized as ABar and C contact in prophase (-5 min) and is internalized during metaphase (-1 min) and anaphase (0 min). Chromosomes are labeled with HIS-48::mCherry; nuclei can be seen in outline from the exclusion of cytosolic SDN-1::GFP. Because we scanned only the dorsal 1/3 of each embryo, ABara is not visible at the onset of anaphase. Embryos expressing the *tjIs57* transgene often display cytosolic mCherry aggregates in ABxx cells (arrows). Genotype: *sdn-1(zh20); juSi99[Pmex-5-SDN-1::GFP-sdn-1 3'UTR]; tjIs57[[Ppie-1-mCherry::HIS-48]*). Scale bar = 10 µm.

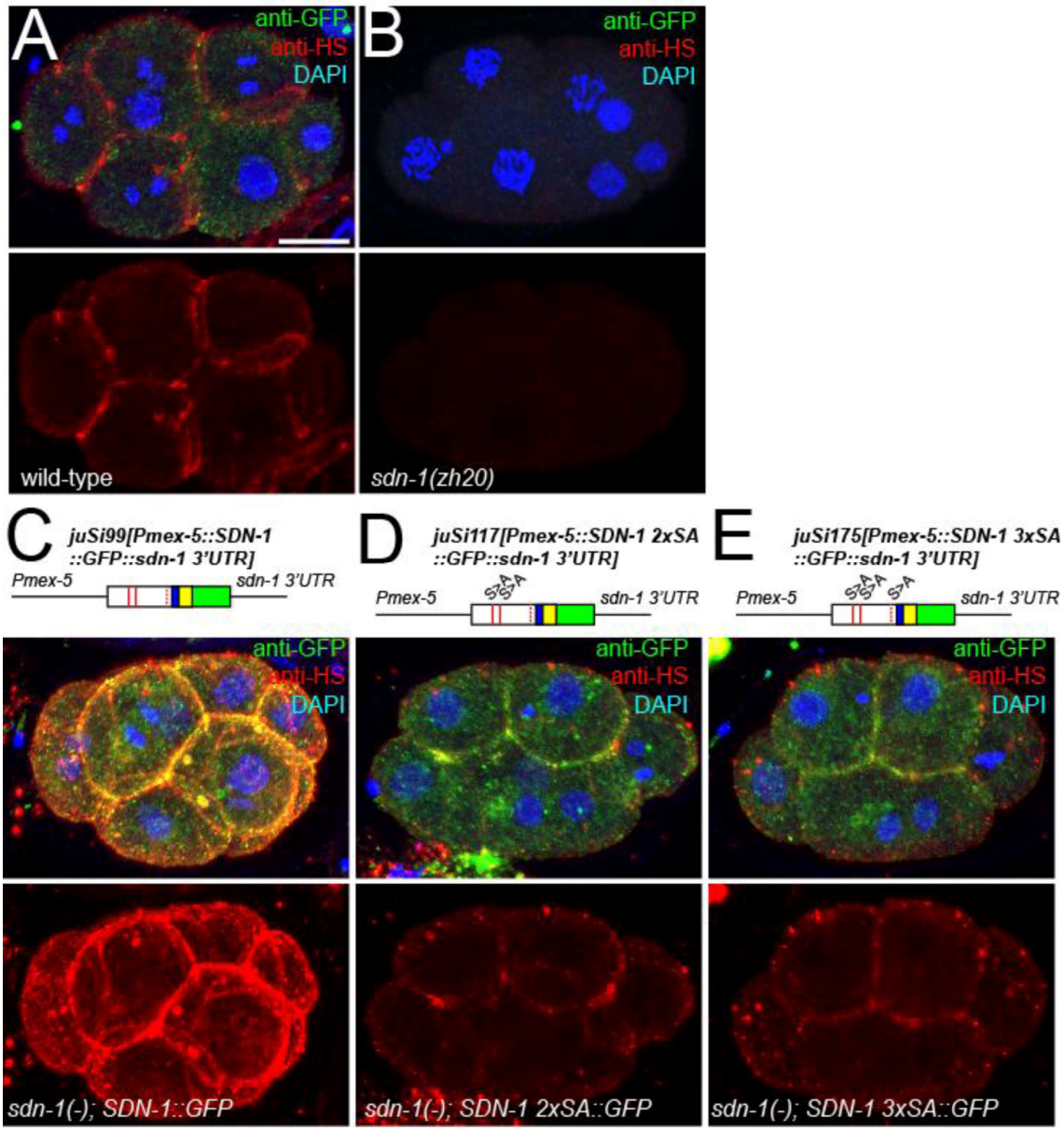

Figure S4. Overexpression of exogenous SDN-1::GFP, SDN-1(2xS>A)::GFP and SDN-1(3xS>A)::GFP can induce 3G10 immunoreactivity in *sdn-1(zh20)*.

Shown are 3D projection images of 6~8-cell stage embryos from (A) wild type, (B) *sdn-1(zh20)*, (C) *sdn-1(zh20); juSi99[Pmex-5-SDN-1::GFP-sdn-1 3'UTR],* (D) *sdn-1(zh20); juSi117[Pmex-5-SDN-1(2xS>A)::GFP-tbb-2 3'UTR]* and (E) *sdn-1(zh20); juSi175[Pmex-5-SDN-1(3xS>A)::GFP-tbb-2 3'UTR]* stained with anti-GFP (green) and 3G10 (red) after heparitinase treatment. Embryos are counter-stained with DAPI (blue). Scale bar = 10 μm.

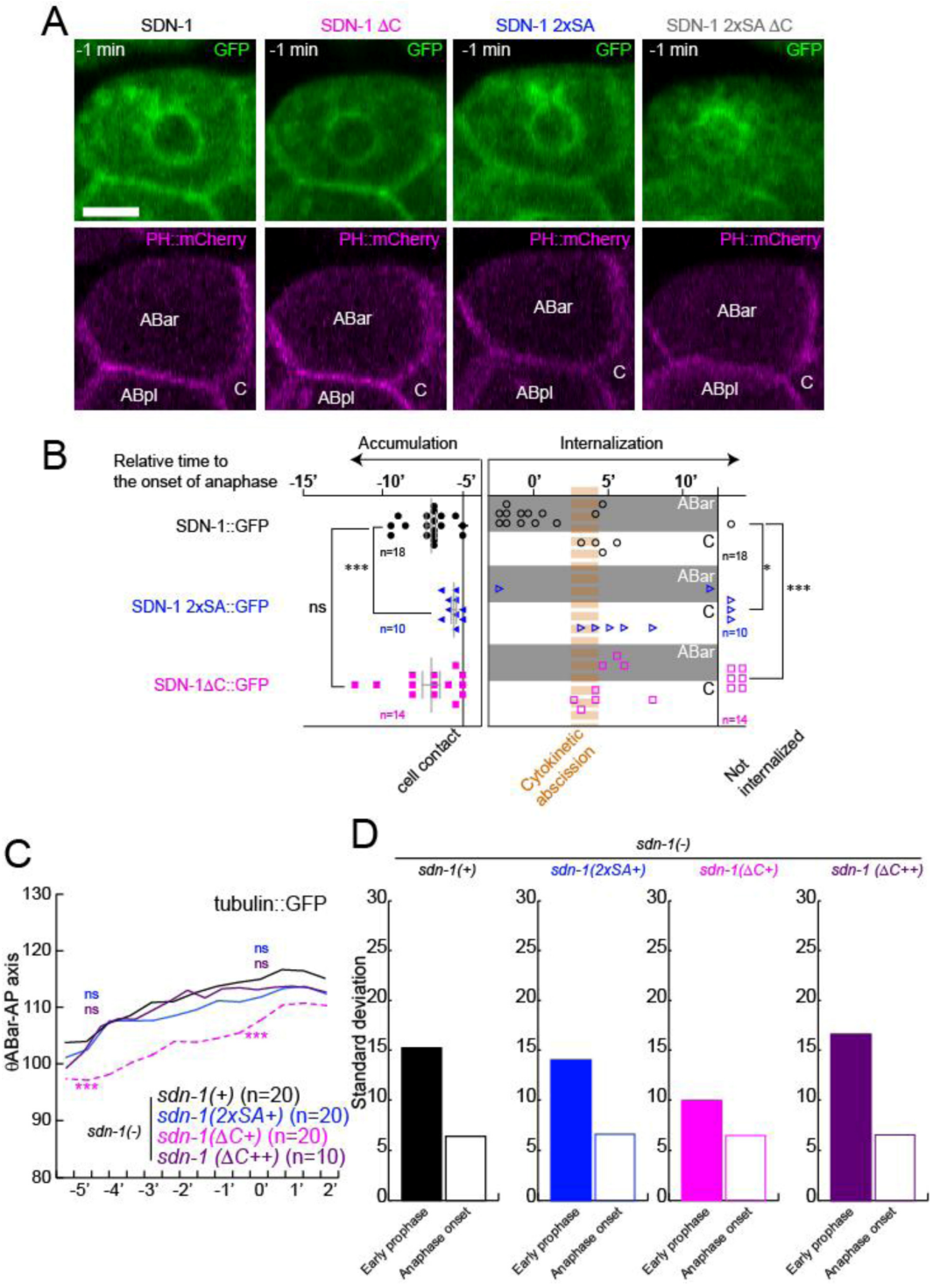

Figure S5. The cytoplasmic domain of SDN-1 is required for SDN-1 internalization during mitosis and for ABar spindle orientation

(A) 3D projection of GFP and PH::mCherry from embryos expressing wild-type SDN-1::GFP (*juSi99*) or mutant forms of SDN-1::GFP (ΔC; *juSi105*, *2xSA*; *juSi117* and *2xSA* ΔC; *juSi144[Pmex-5::SDN-1 2xSA, ΔC::GFP::sdn-1 3'UTR]*) at metaphase (-1 min from the onset of anaphase). SDN-1 2xSA, ΔC::GFP does not show plasma membrane localization.

SDN-1::GFP accumulation is not clearly visible in these panels because the projections were created using a sum of slices to better visualize cytoplasmic GFP. (B) Timing of SDN-1::GFP accumulation and internalization relative to ABar mitosis. Wild type SDN-1::GFP (*mex-5* promoter) begins to accumulate in the 5 minutes preceding contact of ABar and C cells (filled circles). Deletion of the SDN-1 cytoplasmic domain (ΔC) did not affect accumulation dynamics (filled squares); mutation of the SDN-1 GAG attachment sites (2xS>A) significantly delayed accumulation (filled triangles). Wild type SDN-1::GFP was either internalized into ABar during metaphase-anaphase, or less often into C, after cytokinesis. SDN-1ΔC::GFP and SDN-1 2xS>A::GFP both showed delayed internalization. Statistics: Fisher's exact test (before vs after onset of anaphase); *, P<0.05, ***, P<0.001. (C) Wild type SDN-1::GFP (black line) and SDN-1 2xS>A::GFP (blue line) driven by *sdn-1* own promoter and 3'UTR fully rescued the misoriented ABar spindle in *sdn-1(zh20)* mutants. However, SDN-1ΔC::GFP driven by *sdn-1* promoter and 3'UTR did not fully rescue ABar centrosome/spindle orientation relative to the AP axis (dashed pink line). Overexpression of SDN-1ΔC::GFP by *mex-5* promoter and *tbb-2* 3'UTR fully rescued abnormal ABar spindle dynamics in in *sdn-1(zh20)* mutants (purple line). *sdn-1(-), sdn-1(+), sdn-1(C+) and sdn-1(GAG+)* indicate *sdn-1(zh20), juSi119[Psdn-1::SDN-1::GFP::sdn-1 3'UTR], juSi151[Psdn-1-SDN-1ΔC::GFP-sdn-1 3'UTR] and juSi170[Psdn-1-SDN-1 2xS>A::GFP-sdn-1 3'UTR]*, respectively. **, P<0.01, ANOVA, followed by Dunnett test comparing orientation at onset of anaphase. (D) Bar graphs showing standard deviation at early prophase and at onset of anaphase. Variance of spindle orientation at early prophase is not statistically different between these transgenic strains.

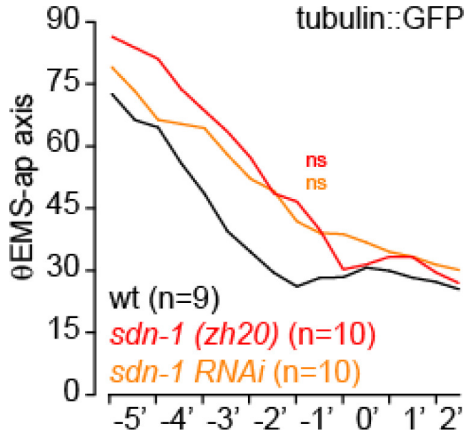

Figure S6. Effects of *sdn-1* loss of function on EMS spindle orientation.

Three dimensional angles between the EMS centrosome axes and AP axis are plotted over time relative to anaphase. Although *sdn-1(zh20)* and *sdn-1* RNAi displayed slight delays in EMS spindle rotation, the mean EMS division angles at -1 min relative to the onset of anaphase are not significantly different.

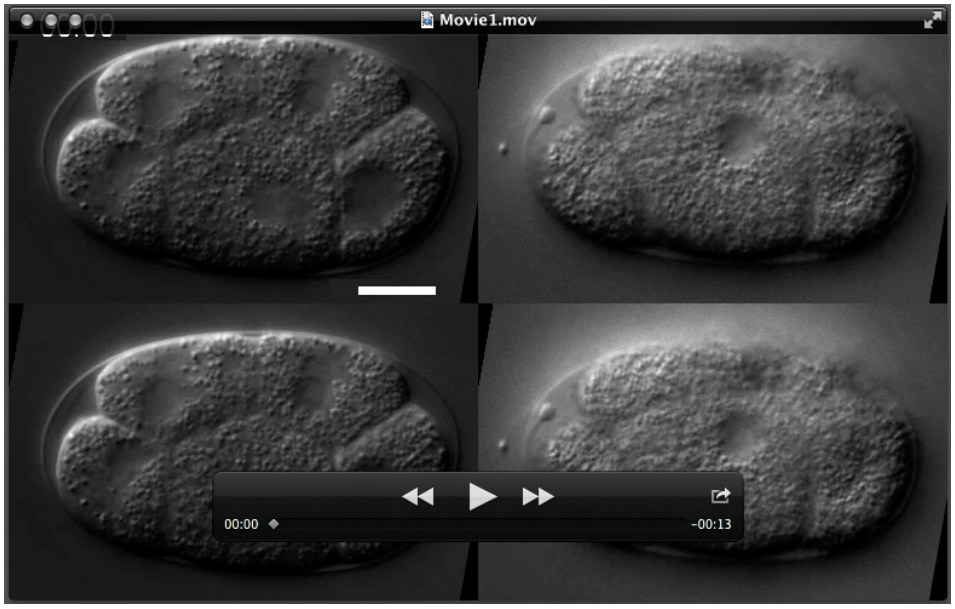
Movie1.mov
00:00
-00:13

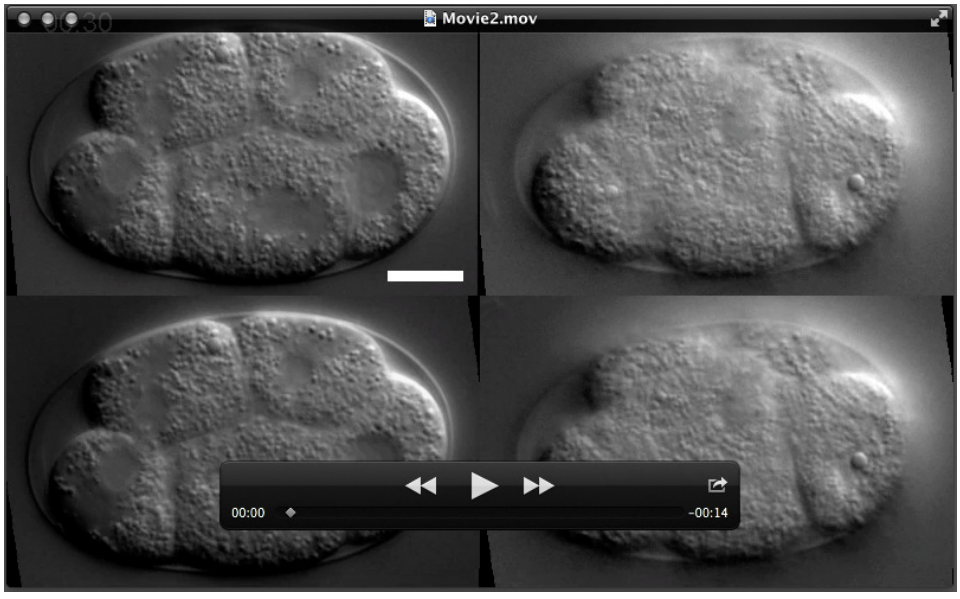
Movie2.mov
00:00
-00:14

Movies 1-3. *sdn-1* mutants and mutants defective in HS synthesis display aberrant ABar cell division orientation.

Differential interference contrast (DIC) imaging of wild-type (Movie 1), *sdn-1(zh20)* (movie 2) and *rib-1(tm516)* (Movie 3) embryos during ABar division. Each movie shows two focal planes from the same 4D movie to display ABar division (left) and ABar-C contact (right). The movie starts in the 6-cell stage and ends at 12-cell stage. Straight lines indicate the orientations of the EMS, ABar, and ABpr divisions. Freehand lines indicate the cell surfaces of ABar (white) and C (green) before and during contact. The cell contact and onset of anaphase in AB granddaughters occur at 06:30~7:00 and 14:00~14:30, respectively. Anterior is left and dorsal is up. Time stamps, min:sec.

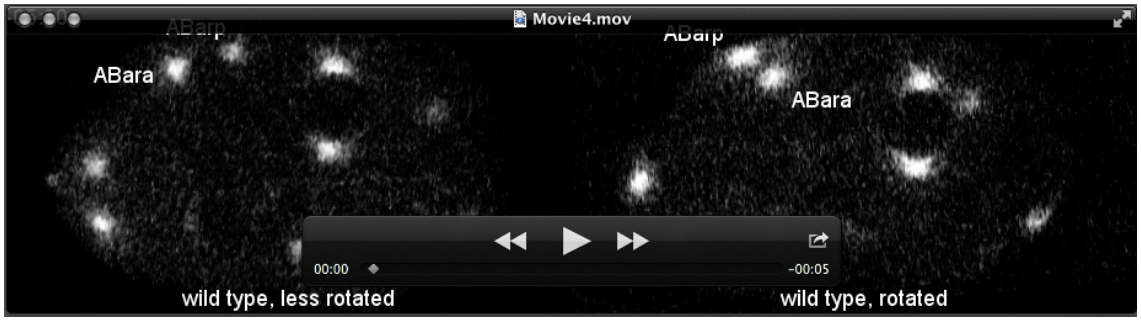

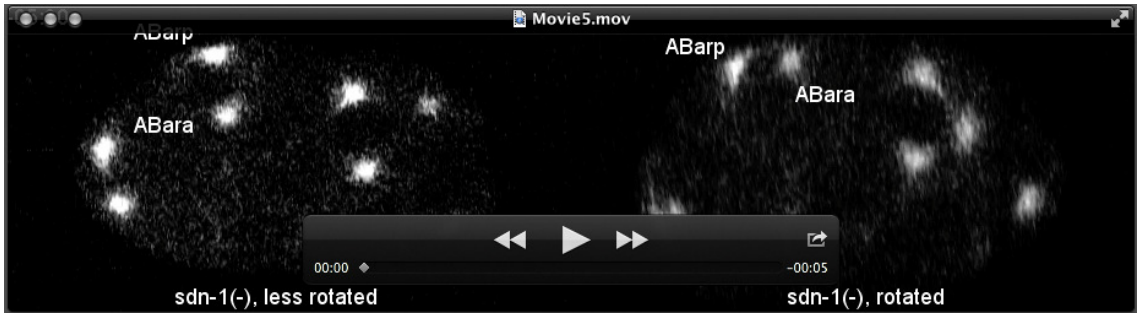

Movies 4, 5. ABar spindle orientation is initially variable in wild-type and in *sdn-1* embryos

Movies of wild type (Movie 4) and of *sdn-1(zh20)* (Movie 5). Each movie shows two representative embryos in which the ABar spindle (marked using TBB-2::GFP) is initially unrotated (i.e. far from its final orientation) left) or is initially in its final orientation (right). Time stamps, min:sec.

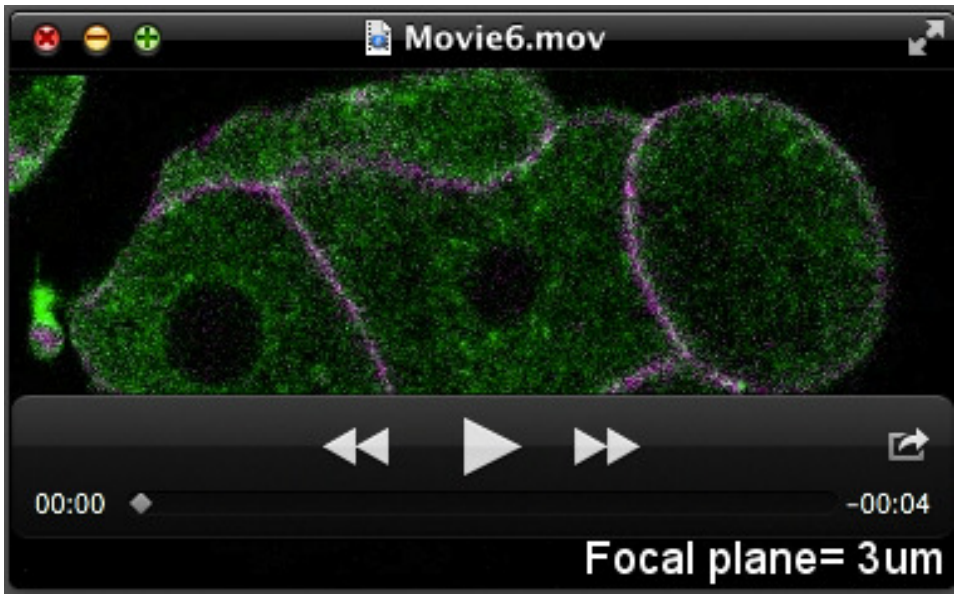

Movie 6. Dynamics of SDN-1::GFP accumulation and colocalization with membrane marker PH::mCherry.

Single focal planes from confocal z-stack movie are shown, moving from 3 µm to 0 µm focal planes (fp) to follow SDN-1::GFP (green) and PH::mCherry (purple). SDN-1::GFP accumulation in ABar is indicated by white arrowheads. Time stamp, min:sec.

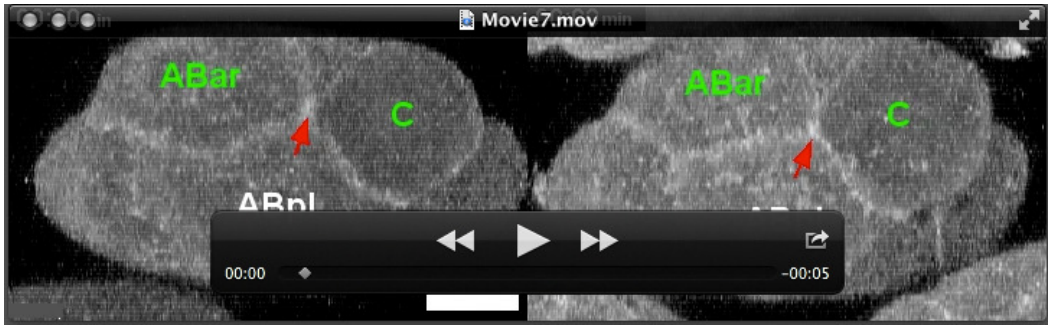

Movie 7. Dynamics of SDN-1::GFP internalization into ABar or into C

3D projection movies of two embryos, one showing that SDN-1::GFP accumulation on the contact site is endocytosed in ABar (left), and one showing internalization into C (right). Red arrows indicate accumulation on the contact while yellow arrows indicate internalization. Time stamp, min:sec.

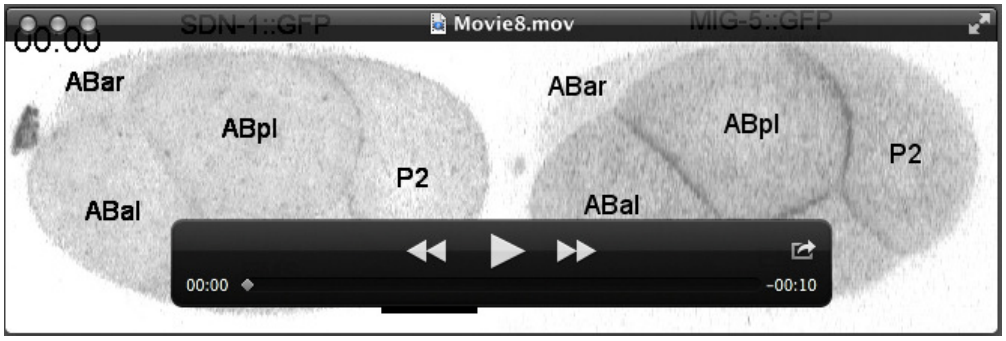

Movie 8. Comparison of the localization dynamics of SDN-1::GFP and MIG-5::GFP.

In the left hand embryo SDN-1::GFP (*juSi98*) accumulation is visible by 8:00 and has begun to internalize by 12:00; ABar anaphase is at 13:00 (double arrow). In the right hand embryo MIG-5::GFP (*juSi138*) accumulation is visible at 9:00. ABar anaphase is at 13:00. Time stamps, min: sec.

Table S1. Strains and Genotypes

Strain Number	Genotype	Allele or Transgene Information (reference)
CZ17609	*zuIs178 V; sdn-1(zh20) X*	*zuIs178* (Ooi et al., 2006), *zh20* (Rhiner et al., 2005)
CZ9752	*zuIs178 V*	
CZ4348	*sdn-1(zh20) X*	
CZ5695	*rib-2(tm710) III/hT2 I;III*	*tm710* (Morio et al., 2003)
CZ5694	*rib-1(tm516) IV/nT1 IV;V*	*tm516* (Kitagawa et al., 2007)
VC758	*hst-1(ok1068) V*	
CZ1742	*rib-1(tm516) IV, zuIs178V/nT1 IV;V*	
CZ17424	*rib-2(tm710)/qC1 III; zuIs178V*	
CZ17425	*hst-1(ok1068)/nT1; zuIs178 IV; V*	*ok1068*
CZ17611	*zuIs178 V; gpn-1(ok377) X*	*ok377* (Hudson et al., 2006)
CZ19260	*juSi98 II; ojIs1*	*juSi98 [Pmex-5-SDN-1cDNA::GFP-tbb-2 3'UTR], ojIs1* (Strome et al., 2001)
CZ19258	*juSi98 II; ojIs1; sdn-1(zh20) X*	
CZ18286	*juSi99 II;sdn-1(zh20) X*	*juSi99[Pmex-5::sdn-1cDNA::gfp::sdn-1 3'UTR]*
CZ19474	*juSi99 II, sdn-1(zh20) X, ltIs44*	*ltIs44[Ppie-1::mCherry::PH(PLC1Δ1)]* (Kachur et al., 2008)
CZ19473	*juSi105 II; ltIs44, sdn-1(zh20) X*	*juSi105[Pmex-5::sdn-1(ΔC)cDNA::gfp::tbb-2 3'UTR]*
CZ19435	*juSi117 II; ltIs44, sdn-1(zh20) X*	*juSi117[Pmex-5::sdn-1(S76A,S81A)cDNA::gfp::sdn-1 3'UTR]*
CZ18427	*juSi119 II*	*juSi119[Psdn-1-SDN-1cDNA::GFP-sdn-1 3'UTR]*
CZ18487	*juSi119 II; zuIs178 V;sdn-1(zh20)*	
CZ18495	*zuIs178 V; sdn-1(ok449) X*	
CZ19255	*juSI138 II*	*juSi138[Pmex-5-MIG-5cDNA::GFP-tbb-2 3'UTR]*
CZ19261	*juSi138 II; sdn-1(zh20) X*	
CZ19482	*juSi117 II; ojIs1;sdn-1(zh20) X*	
CZ19484	*juSi119 II; ojIs1;sdn-1(zh20) X*	
CZ19476	*juSi105 II; ojIs1; sdn-1(zh20) X*	
CZ19259	*ojIs1*	
CZ18681	*ojIs1;sdn-1(zh20) X*	
CZ20383	*juSi151 II; ojIs1; sdn-1(zh20) X*	*juSi151 Pmex-5::sdn-1(ΔC)cDNA::gfp::sdn-1 3'UTR]*
CZ20378	*juSi170 II; ojIs1; sdn-1(zh20) X*	*juSi170[Psdn-1::sdn-1(S76A,S81A, S214A)cDNA::gfp::sdn-1 3'UTR]*
CZ20393	*juSi99 II; sdn-1(zh20) X; tjIs57*	*tjIs57[pie-1p::mCherry::his-48 + unc-119(+)* (Toya et al., 2010)
KD170	*juSi175 II; sdn-1(zh20) X*	*juSi175[Pmex-5::sdn-1(S76A,S81A, S214A)cDNA::GFP::sdn-1 3'UTR]*

OD63	*unc-119(ed3) III; ltIs43/+*	*ltIs43[pAA26; pie-1::GFP-TEV-STag::ZEN-4; unc-119(+)]* (Audhya et al., 2005)
WH279	*unc-119(ed3) III; ojIs12*	*ojIs12 [cyk-4::GFP + unc-119(+)]*(Verbrugghe and White, 2004)

Table S2. Plasmids generated for this study

Plasmid name	contents	Primers used
pCZ839	*Pmex-5-SDN-1::GFP-tbb-2 3'UTR*	PCR #1 (*mex-5* promoter): AC3273 (5'-gactcactagtgggcagatcaaatatcagtttttaaaa -3') and AC3274 (5'-tctctgtctgaaacattcaa -3') PCR #2 (*sdn-1* cDNA): AC3275 (5'-gaatgtttcagacagagaatgattctgaaactcaattt -3') and AC3276 (5'-ccaccacctcctcccgggcacgcgtaaaattcttttgtcg -3') PCR #3 (*gfp::tbb-2* 3'UTR): AC3277 (5'- tgcccgggaggaggtggtgg -3') and AC3276 (5'- ccaccacctcctcccgggcacgcgtaaaattcttttgtcg -3') PCR #4 (vector backbone): AC3278 (5'- tcgaggaattcctgcaggat -3') and AC3279 (5'- gatctgcccactagtgagtc -3')
pCZ840	*Pmex-5-SDN-1::GFP-sdn-1 3'UTR*	PCR #1 (*sdn-1* 3'UTR): AC3288 (5'-tggatgaactatacaaataatctctactgtcatttgttca -3') AC3280 (5'- atcctgcaggaattcctcgataatgtaatatttttatatt -3') PCR #2 (*Pmex-5-SDN-1::GFP*): AC3273 and AC3281 (5'-ttatttgtatagttcatcca -3') PCR #3 (vector backbone): AC3278 and AC3279
pCZ841	*Pmex-5-SDN-1ΔC::GFP::tbb-2 3'UTR*	PCR #1 (*mex-5* promoter): AC3273 and AC3274 PCR #2 (*sdn-1* ΔC cDNA): AC3275 and AC3282 (5'-gttcttctcctttactcatgactacaaagagcacgagtagaa -3') PCR #3 (*gfp::tbb-2* 3'UTR): AC3277 and AC3276 PCR #4 (vector backbone): AC3278 and AC3279
pCZ843	*Pmex-5-SDN-1(S71A, S86A)::GFP-sdn-1 3'UTR*	AC3259 (5'-tgatgtccatggggcaggcaagccgcc-3') and AC3260 (5'-ggcggcttgcctgccccatggacatca-3') for Ser86Ala AC3272 (5'-gcagacatcgaagtcaatggagccggctaccca-3') and AC3273 (5'-tgggtagccggctccattgacttcgatgtctgc-3') for Ser71Ala
pCZ844	*Pmex-5-MIG-5::GFP-tbb-2 3'UTR*	PCR#1 (mig-5 cDNA): AC3285 (5'-ttgaatgtttcagacagagaatggagccgccatgcac -3') and AC3286 (5'-ccaccacctcctcccgggcaagtccgtaaaatacgcgttc -3') PCR#2 (vector backbone): AC3278 and AC3279
pCZ838	*Psdn-1-SDN-1::GFP-sdn-1 3'UTR*	PCR #1 (*sdn-1* promoter): AC3283 (5'-actcactagtgggcagatcagcgcgtaacgcaaactatt -3') and AC3284 (5'-attgtcttgttggtgtaatcacctg -3') PCR #2 (vector): AC3287(5'-gattacaccaacaagacaatatgattctgaaactcaatttctgcct -3') and AC3279
pCZ861	*Pmex-5_sdn1_deltaGAG3x_sdn-1 3UTR*	AC3646 (5'- atctcagctggaccattctcgccattc -3') and AC3647 (5'-tggtccagctgagatggttgatgtgac -3') for Ser214Ala

Table S3. Primer list for dsRNA synthesis and real-time qPCR

Template for	Primers (T7 promoter sequence is underlined.)
dsh-2 dsRNA	AC3289 5'-taatacgactcactatagggatgacagattccccttcacc-3' AC3290 5'-taatacgactcactatagggtgacaccgtctcggtaatga-3'
mig-5 dsRNA	AC3291 5'-taatacgactcactatagggatggagccgccatgcacatc-3' AC3292 5'-taatacgactcactatagggaggatgcagcttctctgagc-3'
mom-2 dsRNA	AC3295 5'-taatacgactcactatagggatgcacatcaacacgccagt-3' AC3296 5'-taatacgactcactatagggtttggtgaagcatccaggt-3'
src-1 dsRNA	AC3293 5'-taatacgactcactatagggatgggttgcctgttttcaaa-3' AC3294 5'-taatacgactcactatagggaatcgccacctcaacaattc-3'
sdn-1 dsRNA	AC3297 5'-taatacgactcactatagggatgattctgaaactcaatttctgcc-3' AC3298 5'-taatacgactcactatagggcgaggcatatggtcttgctt-3'
wrm-1 dsRNA	kpr303 5'- taatacgactcactatagggatggatgtggattgcgcagaaac -3' kpr304 5'- taatacgactcactatagggcacattagttgtcgatgatgctgc -3'

References for Supplementary Materials

Audhya, A., Hyndman, F., McLeod, I. X., Maddox, A. S., Yates, J. R., 3rd, Desai, A. and Oegema, K. (2005). A complex containing the Sm protein CAR-1 and the RNA helicase CGH-1 is required for embryonic cytokinesis in *Caenorhabditis elegans*. *J Cell Biol* **171**, 267-79.

Hudson, M. L., Kinnunen, T., Cinar, H. N. and Chisholm, A. D. (2006). *C. elegans* Kallmann syndrome protein KAL-1 interacts with syndecan and glypican to regulate neuronal cell migrations. *Dev Biol* **294**, 352-65.

Kachur, T. M., Audhya, A. and Pilgrim, D. B. (2008). UNC-45 is required for NMY-2 contractile function in early embryonic polarity establishment and germline cellularization in *C. elegans*. *Dev Biol* **314**, 287-99.

Kitagawa, H., Izumikawa, T., Mizuguchi, S., Dejima, K., Nomura, K. H., Egusa, N., Taniguchi, F., Tamura, J., Gengyo-Ando, K., Mitani, S. et al. (2007). Expression of *rib-1*, a *Caenorhabditis elegans* homolog of the human tumor suppressor EXT genes, is indispensable for heparan sulfate synthesis and embryonic morphogenesis. *J Biol Chem* **282**, 8533-44.

Morio, H., Honda, Y., Toyoda, H., Nakajima, M., Kurosawa, H. and Shirasawa, T. (2003). EXT gene family member *rib-2* is essential for embryonic development and heparan sulfate biosynthesis in *Caenorhabditis elegans*. *Biochem Biophys Res Commun* **301**, 317-23.

Ooi, S. L., Priess, J. R. and Henikoff, S. (2006). Histone H3.3 variant dynamics in the germline of *Caenorhabditis elegans*. *PLoS Genet* **2**, e97.

Rhiner, C., Gysi, S., Frohli, E., Hengartner, M. O. and Hajnal, A. (2005). Syndecan regulates cell migration and axon guidance in *C. elegans*. *Development* **132**, 4621-33.

Strome, S., Powers, J., Dunn, M., Reese, K., Malone, C. J., White, J., Seydoux, G. and Saxton, W. (2001). Spindle dynamics and the role of gamma-tubulin in early *Caenorhabditis elegans* embryos. *Mol Biol Cell* **12**, 1751-64.

Toya, M., Iida, Y. and Sugimoto, A. (2010). Imaging of mitotic spindle dynamics in *Caenorhabditis elegans* embryos. *Methods Cell Biol* **97**, 359-72.

Verbrugghe, K. J. and White, J. G. (2004). SPD-1 is required for the formation of the spindle midzone but is not essential for the completion of cytokinesis in *C. elegans* embryos. *Curr Biol* **14**, 1755-60.